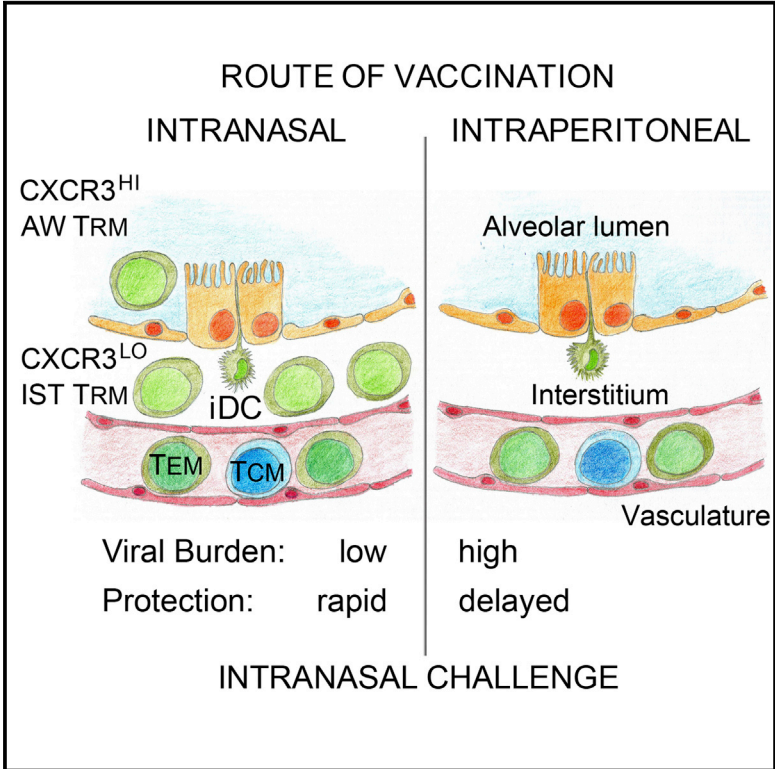


A Distinct Lung-Interstitial-Resident Memory CD8⁺ T Cell Subset Confers Enhanced Protection to Lower Respiratory Tract Infection

Graphical Abstract



Authors

Pavlo Gilchuk, Timothy M. Hill, Clifford Guy, ..., Eric Sebzda, Douglas R. Green, Sebastian Joyce

Correspondence

sebastian.joyce@vanderbilt.edu

In Brief

Mucosal surveillance ensures rapid protection when a pathogen breaches the barrier. Gilchuk et al. report that local vaccination elicits a distinct resident memory CD8⁺ T cell subset that localizes to the lung interstitium. These T cells protect against respiratory infections by positioning at vulnerable sites and acting quickly against infections.

Highlights

- Intranasal T cell epitope-targeted vaccination confers enhanced protection
- Intranasal vaccination preferentially induces CXCR3^{LO} lung-resident memory CD8⁺ T cells
- Protective memory T cells localize to vulnerable sites of the lung interstitium
- Interstitial memory CD8⁺ T cells rapidly protect the lung against infection

A Distinct Lung-Interstitial-Resident Memory CD8⁺ T Cell Subset Confers Enhanced Protection to Lower Respiratory Tract Infection

Pavlo Gilchuk,^{1,2} Timothy M. Hill,^{2,7} Clifford Guy,⁵ Sean R. McMaster,⁶ Kelli L. Boyd,² Whitney A. Rabacal,² Pengcheng Lu,^{3,4} Yu Shyr,³ Jacob E. Kohlmeier,⁶ Eric Sebzda,² Douglas R. Green,⁵ and Sebastian Joyce^{1,2,8,*}

¹Department of Veterans Affairs Tennessee Valley Healthcare System, Nashville, TN 37232, USA

²Department of Pathology, Microbiology and Immunology

³Vanderbilt Technologies for Advanced Genomics Analyses and Research Design

⁴Department of Biostatistics

Vanderbilt University School of Medicine, Nashville, TN 37232, USA

⁵Department of Immunology, St. Jude Children's Research Hospital, Memphis, TN 38105, USA

⁶Department of Microbiology and Immunology, Emory University School of Medicine, Atlanta, GA 30322, USA

⁷Present address: Department of Chemistry & Life Science, United States Military Academy, West Point, NY 10996, USA

⁸Lead Contact

*Correspondence: sebastian.joyce@vanderbilt.edu

<http://dx.doi.org/10.1016/j.celrep.2016.07.037>

SUMMARY

The nature and anatomic location of the protective memory CD8⁺ T cell subset induced by intranasal vaccination remain poorly understood. We developed a vaccination model to assess the anatomic location of protective memory CD8⁺ T cells and their role in lower airway infections. Memory CD8⁺ T cells elicited by local intranasal, but not systemic, vaccination with an engineered non-replicative CD8⁺ T cell-targeted antigen confer enhanced protection to a lethal respiratory viral challenge. This protection depends on a distinct CXCR3^{LO} resident memory CD8⁺ T (T_{RM}) cell population that preferentially localizes to the pulmonary interstitium. Because they are positioned close to the mucosa, where infection occurs, interstitial T_{RM} cells act before inflammation can recruit circulating memory CD8⁺ T cells into the lung tissue. This results in a local protective immune response as early as 1 day post-infection. Hence, vaccine strategies that induce lung interstitial T_{RM} cells may confer better protection against respiratory pathogens.

INTRODUCTION

Memory of past encounters with pathogens is a key feature of the adaptive immune system and the basis for successful vaccination. Antigen-specific memory CD8⁺ T cells play key roles in protection against infectious diseases. A delay in the generation of effector CD8⁺ T cells and/or the recall of circulating memory CD8⁺ T cells to the site of infection allows pathogens to replicate and cause disease. Non-circulating tissue-resident memory CD8⁺ T (T_{RM}) cells, by virtue of their optimal positioning at bar-

riers (e.g., skin, intestine, female reproductive tract, and respiratory tract), keep infections in check at sites of pathogen entry to confer protective immunity (Ariotti et al., 2012; Bergsbaken and Bevan, 2015; Bivas-Benita et al., 2013; Hickman et al., 2015; Jiang et al., 2012; Li et al., 2013; Mackay et al., 2013; Salek-Ardakani et al., 2011; Schenkel et al., 2014; Sheridan et al., 2014; Shin and Iwasaki, 2012; Slütter et al., 2013; Takamura et al., 2010). Hence, insights into the generation and function of T_{RM} cells are essential for devising ways to induce protective immunity by vaccination (Clark, 2015; Schenkel and Masopust, 2014).

The respiratory mucosa is a major site for pathogen invasion and, hence, a site for constant immune surveillance. Safeguarding the lungs (especially the terminal respiratory tree that consists of alveoli and associated capillary beds) from injury is critical to preserve lung function. Thus, severe morbidity and mortality in respiratory infectious diseases are associated with viral dissemination and inflammation, which can damage the lung parenchyma and alveoli (Gilchuk et al., 2013; Manicassamy et al., 2010). To protect from disease, memory CD8⁺ T cells are strategically distributed within distinct anatomical compartments of the lungs (Hasenberg et al., 2013; Lelkes et al., 2014; Rangel-Moreno et al., 2011). The anatomical niche that memory CD8⁺ T cells occupy in the lungs depends on the route of infection (Anderson et al., 2012). Nonetheless, the precise location and protective capacity of different CD8⁺ T_{RM} cell subsets in the lungs that are elicited by vaccination are poorly understood.

Most vaccines in clinical use, including those protecting against respiratory infections, are administered to elicit systemic rather than local immune responses. Live and attenuated microbes are dangerous for use as pulmonary vaccines, and inactivated microbes poorly elicit cellular immunity. Consequently, there is a need for physiologically relevant experimental models that closely recapitulate protective CD8⁺ T_{RM} cell responses to vaccination in the lungs. Here, we describe a model in which lower airway vaccination with a non-replicative pathogen-derived protein antigen elicits high frequency of epitope-specific

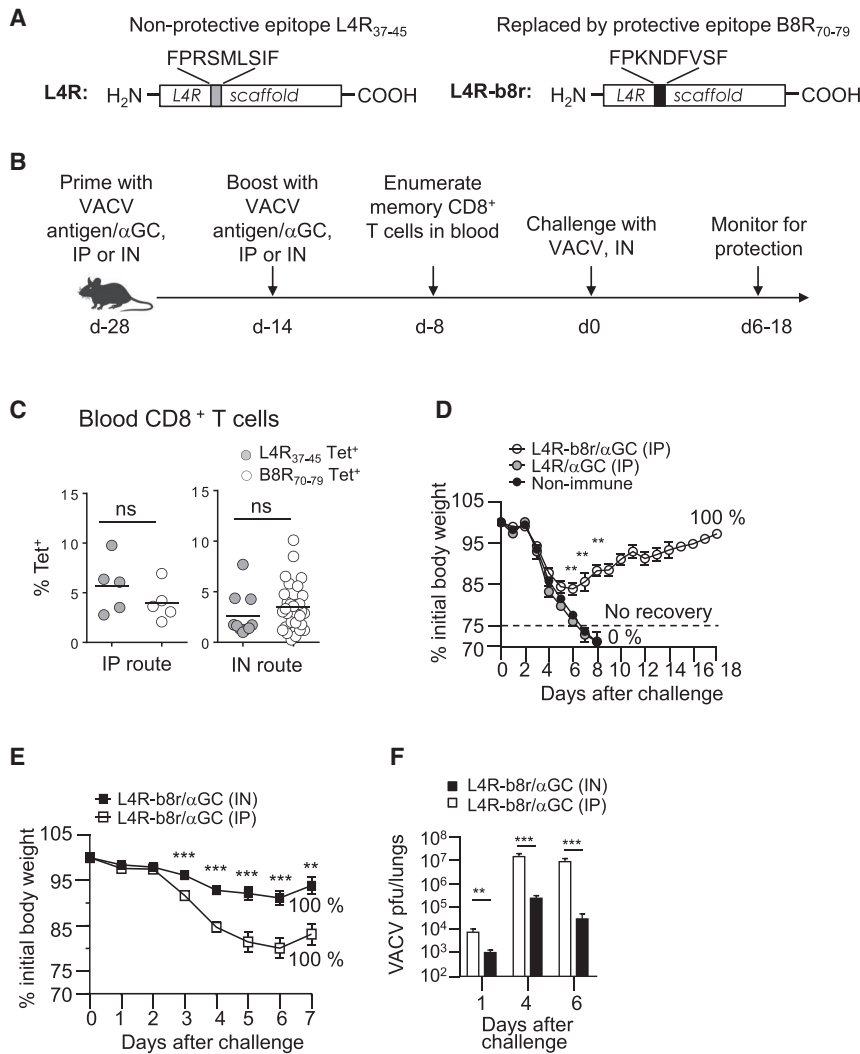


Figure 1. Intranasal Vaccination with CD8⁺-Targeted Antigenic Protein and αGC Confers Enhanced Protection from Respiratory Virus Infection

Protein antigen was formulated with αGC and administered to mice by the intraperitoneal or IN route. Vaccinated mice were challenged with VACV and assessed for protection.

(A) Design of immunogens used in vaccination.

(B) Prime and boost vaccination approach.

(C) Frequency of epitope-specific CD8⁺ T cells was enumerated on day 6 after boost in blood using the corresponding tetramers. Each symbol indicates an individual mouse.

(D) Protection of mice that were IP vaccinated with αGC-formulated L4R or L4R-b8r protein antigens.

(E) Protection of mice that were IP or intranasally vaccinated with L4R-b8r plus αGC.

(F) VACV burden in the lungs was measured on days 2, 4, and 6 p.i. in mice vaccinated as in (E); n = 5–21 mice/group, mean ± SEM; number indicates percent survival based on endpoint criteria. See also Figure S1.

VACV-derived proteins (L4R and L4R-b8r). To create L4R-b8r, the native non-protective L4R₃₇₋₄₅ peptide in L4R was substituted with the protective B8R epitope. Thus, L4R and L4R-b8r are made of the same protein scaffold but differ only in the epitope they contain (Figure 1A).

To test the immunogenicity of L4R and L4R-b8r, HLA-B7.2 transgenic (B7.2^{tg}) mice were primed and boosted intraperitoneally (IP) (Figure 1B) with the protein antigen formulated with α-galactosylceramide (αGC) as the adjuvant (Gilchuk et al., 2013; Semmling et al., 2010). Staining

with the corresponding B7.2-peptide tetramer (Tet) showed that both protein antigens induced a robust systemic CD8⁺ T cell response (Figure 1C). The response was specific to the epitope used for immunization, because the elicited CD8⁺ T cells reacted only with the cognate tetramer (Figure S1). Moreover, under conditions promoting severe lower airway infection, intraperitoneal vaccination with L4R-b8r was sufficient to protect mice from a lethal respiratory VACV challenge, while L4R-vaccinated mice succumbed to disease (Figure 1D). Thus, B8R-specific CD8⁺ T cells were the sole mediators of protection, with undetectable contribution by other adaptive immune cells to the antigen or the adjuvant. We next compared the protective potential of memory B8R-specific CD8⁺ T cells generated by intraperitoneal and intranasal (IN) vaccinations. Strikingly, intranasally vaccinated mice lethally challenged with VACV were more resistant to disease and showed lower VACV titers in the lung as early as day 1 post-infection (p.i.) (Figures 1E and 1F). We concluded that IN vaccination, when compared to intraperitoneal vaccination, with CD8⁺ T cell-targeted antigen more efficiently protected mice from lethal respiratory VACV infection.

RESULTS

Intranasal Vaccination with Antigenic Protein Plus Adjuvant Confers Enhanced Protection against Respiratory Virus Infection

We previously reported two HLA-B7.2-restricted VACV-derived CD8⁺ T cell epitopes: B8R₇₀₋₇₈ (B8R), which elicited a protective polyclonal CD8⁺ T cell response upon peptide vaccination; and L4R₃₇₋₄₅, which elicited a robust CD8⁺ T cell response but was non-protective for reasons previously reported (Gilchuk et al., 2013). This finding was exploited to dissect the protective capabilities of endogenous (non-T cell receptor [TCR] transgenic), epitope-specific CD8⁺ T cells. We engineered two recombinant

CD8⁺ T_{RM} cells within the lung tissue that conferred rapid protection to mice against lethal vaccinia virus (VACV) infection of the lower respiratory tract. A comparative analysis of the outcomes of distinct vaccination routes revealed that the protective CD8⁺ T_{RM} cell subset localized to a spatially distinct niche within the lung parenchyma and exhibited unique phenotypic features.

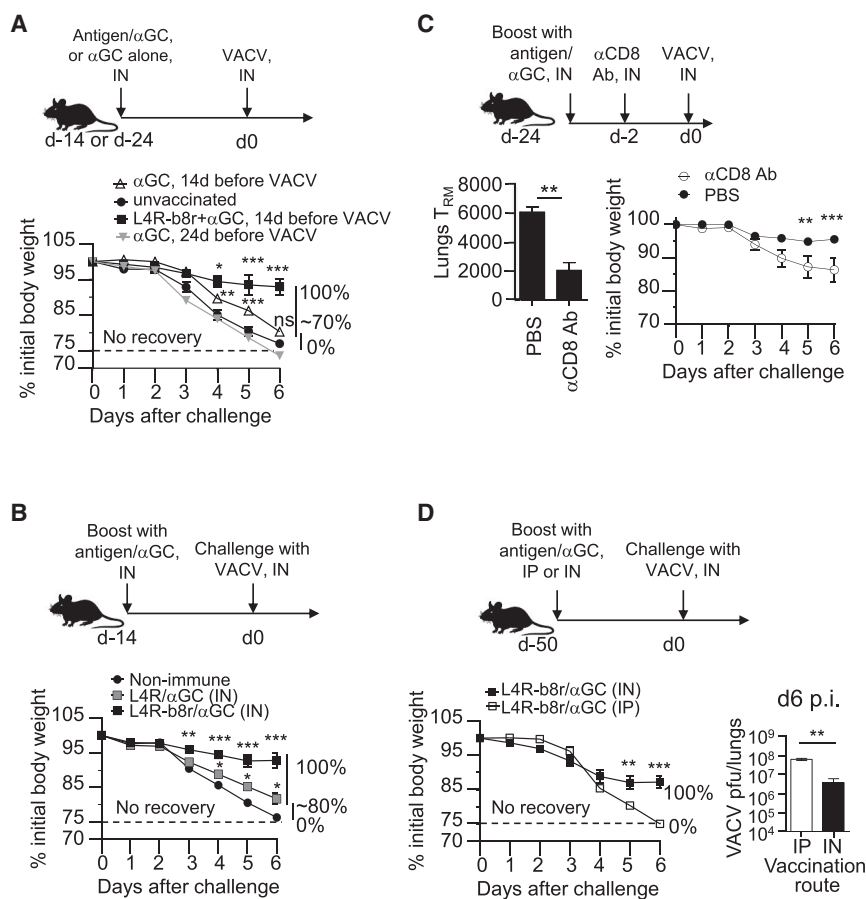


Figure 2. Epitope-Specific CD8⁺ T Cells Participate in Enhanced Protection and Long-Term Immunity

(A and B) Protection of mice that were treated intranasally with α GC alone (A) or L4R plus α GC (B) before lethal challenge with VACV. (C) Protection of intranasally vaccinated mice that received 5 μ g α CD8 Ab or PBS (mock) intranasally and challenged 48 hr later with a lethal dose of VACV. TRM cells were assessed in the lungs of both groups at 24 hr after the treatment using IV staining. (D) Protection of mice that were vaccinated intranasally with L4R-b8R plus α GC and challenged with VACV on day 50 after boost. Data are pooled from two or more independent experiments using $n = 3$ or more mice/group (A and B). One of two independent experiments for (C) and (D), $n = 3$ –14 mice/group; mean \pm SEM. Number indicates percent survival based on endpoint criteria. See also Figure S2.

α CD45 Ab⁺; Figures 2C and S2C–S2E). This depletion rendered otherwise resistant intranasally vaccinated mice more susceptible to respiratory VACV challenge (Figures 2C and S2C–S2E), showing that lung TRM cells participate in protection.

Finally, we investigated the duration of protection by memory CD8⁺ T cells elicited after intraperitoneal or IN vaccination. Notably, only intranasally vaccinated and not IP-vaccinated mice were protected when challenged intranasally with VACV at day 50 after boost, suggesting a key role for IN vaccination in establishing long-lasting protective immunity (Figure 2D). These data together established a non-TCR transgenic mouse model to study the basis of immune protection rendered against lethal respiratory infection by endogenous lung CD8⁺ TRM cells.

Epitope-Specific CD8⁺ T Cells Elicited by Protein Vaccination Mediate Long-Term Protection against Lethal Virus Infection

IN α GC administration rapidly induces local inflammatory responses and interferon- γ (IFN- γ) production (Courtney et al., 2011), potentially explaining the enhanced protection observed when α GC was used as an adjuvant. To investigate antigen specificity of the observed protective immune responses, we primed and boosted mice intranasally with α GC alone or with α GC plus L4R-b8r and then challenged them with VACV on day 14 or on day 24 after boost. We chose day 24 after boost because α GC-induced IFN- γ responses in the lungs wane substantially by then (Courtney et al., 2011). We found that IN α GC treatment 14 days before challenge played very little role in conferring protective immunity that waned after 3 weeks. (Figures 2A, 2B, S2A, and S2B). Thus, B8R-specific CD8⁺ T cells in the lungs participate in enhanced protection to respiratory infection.

To directly demonstrate that CD8⁺ T cells elicited upon IN vaccination participated in protection, we locally depleted them by IN α CD8 antibody (Ab) delivery (Slütter et al., 2013). Lung TRM cells were quantified after intravascular (IV) staining with α CD45 Ab *in vivo* to identify circulating blood leucocytes (Anderson et al., 2014). Local CD8⁺ T cell depletion significantly decreased the number of CD8⁺ TRM cells in the lungs (Tet⁺ α CD45 Ab⁻) but maintained intravascular CD8⁺ T cells (Tet⁺

Intranasal Vaccination Elicits a Distinct CXCR3^{LO} CD8⁺ TRM Cell Subset in the Lung Interstitium

We next investigated the immunologic properties of B8R-specific CD8⁺ T cells elicited by intraperitoneal or IN vaccination. We found that both immunization routes elicited robust systemic and local pulmonary memory CD8⁺ T cell responses of comparable frequency (Figure 3A). B8R-specific CD8⁺ T cells elicited by both vaccination routes responded to antigen by producing IFN- γ and mobilizing CD107a to the cell surface (Figures S3A and S3B). Upon IN VACV challenge, a higher frequency of responding B8R-specific CD8⁺ T cells was found in the lungs of IP-vaccinated mice when compared to those of intranasally vaccinated mice (Figures S3C and S3D). Hence, the frequency of antigen-specific CD8⁺ T cells capable of producing IFN- γ and degranulate fail to explain why IN vaccination enhances protective immunity.

The airways and the lung parenchyma are composed of specialized immunological niches (Hasenberg et al., 2013)

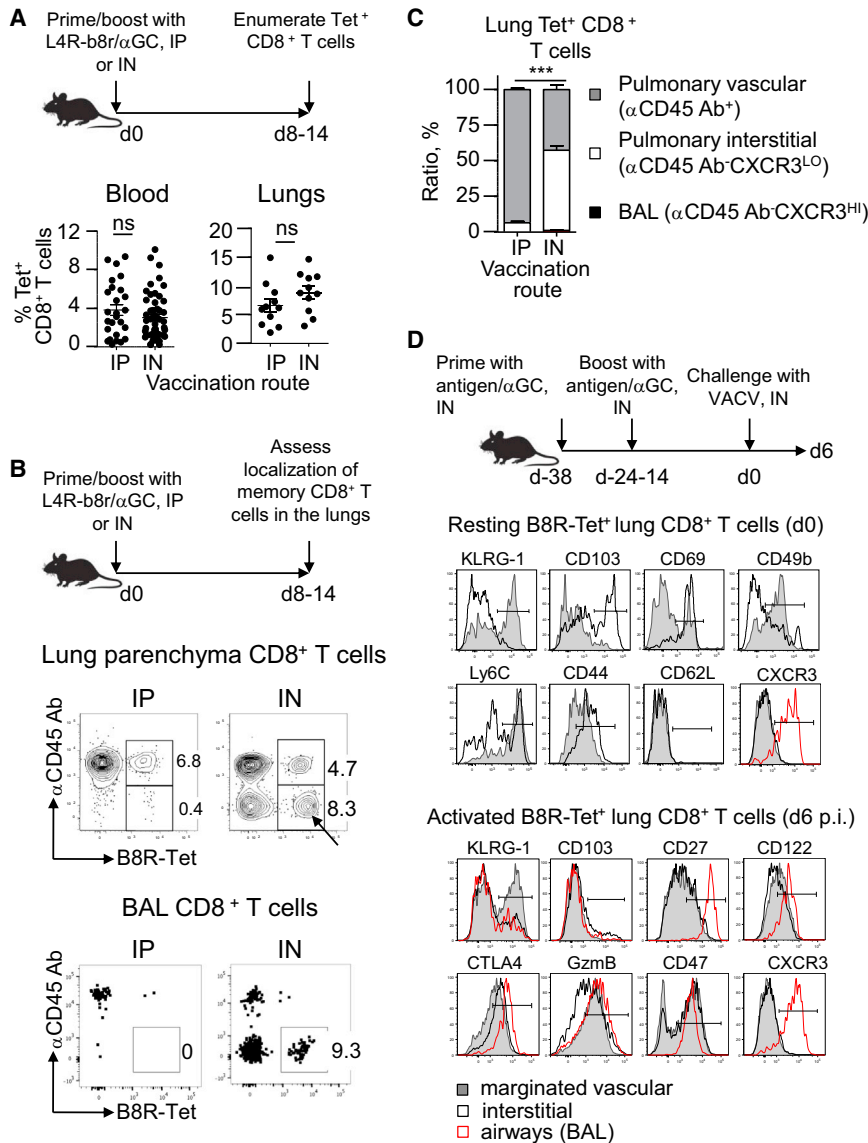


Figure 3. IN Vaccination Elicits Distinct CXCR3^{LO} CD8⁺ T_{RM} Cells that Are Enriched in the Lung Interstitium

(A) B8R-specific CD8⁺ T cell frequency enumerated in blood days 4–6 after boost, or in lungs on days 7–10 after boost.

(B and C) Partitioning (B) and ratio (C) of memory CD8⁺ T cells in the lung parenchyma and BAL of IP- or intranasally vaccinated mice assessed by in vivo staining by intravenous αCD45 Ab delivery followed by ex vivo tetramer staining. Plots are gated on viable CD8⁺ T cells; the arrow indicates interstitial T_{RM} (Tet⁺ IV αCD45 Ab⁻) that are enriched in the lung parenchyma of intranasally vaccinated mice.

(D) Phenotype of resting (days 14–24 after IN boost) or VACV-activated B8R-specific lung CD8⁺ T cells assessed after IV staining. Resting AW T_{RM} cells were assessed only for CXCR3 due to their low number. Data are pooled from three or more independent experiments using n = 3 or more mice/group and represented as mean ± SEM. See also Figures S3 and S4.

sific CD8⁺ T cells were located within the lung interstitium (Tet⁺ αCD45 Ab⁻), vasculature (Tet⁺ αCD45 Ab⁺), and airways (Tet⁺ αCD45 Ab⁻). Remarkably, IST T_{RM} cells comprised a large fraction (>50%) and AW T_{RM} cells represented only a minor fraction (<2%) of total memory CD8⁺ T cells in the lungs (Figures 3B and 3C). Thus, local antigen exposure and inflammation are critical for generating and maintaining a high frequency of IST T_{RM} cells in the lungs.

The frequency of MV and IST CD8⁺ T cells in perfused lungs was >3- to 10-fold higher than in the blood or lung-associated lymph nodes (LNs) (Figures S4A and S4B). Hence, the MV and IST memory CD8⁺ T cells detected in this study

suggesting that local versus systemic vaccination results in differential localization of memory CD8⁺ T cells within the lungs. By staining with αCD45 Ab in vivo and with αCD8 Ab and Tet ex vivo, the distribution of airway (AW)-resident CD8⁺ T cells in bronchoalveolar lavage (BAL) and parenchymal CD8⁺ T cells in two anatomically distinct compartments of the lungs (the vasculature [“margined” vascular (MV)] and interstitium [interstitial (IST)]) were assessed in response to the two immunization routes. We found that the Tet⁺ αCD45 Ab⁻ CD8⁺ T cells of the BAL and lung parenchyma were attributed to AW and IST T_{RM} cells, respectively (Figure 3B), as previously suggested by others (Anderson et al., 2014; Barletta et al., 2012).

Most B8R-specific CD8⁺ T cells (>95%), after intraperitoneal immunization but prior to challenge were Tet⁺ αCD45 Ab⁺ representing the MV memory pool confined to the lung vasculature (Figures 3B and 3C). In contrast, after IN immunization, B8R-spe-

were confined to lung parenchyma and were not blood or LN contaminants. Tet⁺ αCD45 Ab⁻ T_{RM} cells recovered from the BAL uniformly expressed CXCR3^{HI}, a marker for AW T_{RM} cells (Kohlmeier et al., 2009; Slütter et al., 2013). In contrast, Tet⁺ αCD45 Ab⁻ T_{RM} cells retained in the lung parenchyma after perfusion were CXCR3^{LO}, suggesting no cross-contamination between AW and IST T_{RM} cells (Figure S4C).

Resting IST T_{RM} cells were composed of CD103^{HI} and CD103^{LO/NEG} subsets that expressed higher levels of CD69 and CD44 than MV CD8⁺ T cells and were KLRG1^{LO}, CD62L^{LO}, CCR7^{LO}, CD122^{LO}, and CD127^{HI}, a phenotype consistent with the current definition of a T_{RM} cell (Figure 3D). Unlike CXCR3^{HI} AW T_{RM} cells, IST T_{RM} cells were CXCR3^{LO}, thereby discriminating between the two T_{RM} cell subsets in the lungs (Figures 3D and S4C). Resting and activated IST T_{RM} cells were responsive to re-stimulation with antigenic peptide and stained for GzmB ex vivo (Figure 3D; data not shown). Thus, IN

immunization with a non-replicative immunogen and α GC elicited functionally competent and CXCR3^{LO} memory CD8⁺ T cells that occupied a distinct anatomical niche in immune lungs and acquired a tissue resident phenotype.

IST T_{RM} Cells Persist in the Lungs and Respond before Systemic Memory CD8⁺ T Cells Are Recruited to the Site of Infection

We next determined the prevalence of B8R-specific CD8⁺ T cells within the lung parenchyma and BAL after intraperitoneal or IN vaccination and during infection (Figure 4A). Regardless of the vaccination route, similar numbers of MV Tet⁺ CD8⁺ T cells were detected in the lungs at day 14 post-boost and until day 4 after lethal IN VACV challenge. Strikingly, at the same time points there were ~15- to 40-fold higher numbers of IST T_{RM} cells in intranasally vaccinated lungs as compared to IP-immunized lungs (Figure 4A). Moreover, IN vaccination established $\sim 3 \times 10^4$ IST T_{RM} cells per lung, which accounted for >98% of total lung CD8⁺ T_{RM} cells during early infection. This IST T_{RM} cell number is likely an underestimate, owing to dramatic cell losses (>98%) incurred during tissue processing (Steinert et al., 2015). IN immunization also induced ~ 500 AW CD8⁺ T_{RM} cells per lung, which were undetectable in IP-immunized mouse lungs (Figure 4A). This small population of AW T_{RM} cells was sustained in the airways without substantial change in number until day 6 p.i. The dramatically higher number of pre-existing IST T_{RM} cells present during early infection was associated with the rapid reduction of viral load in intranasally vaccinated mice. Conversely, the delayed accumulation of IP-induced memory CD8⁺ T cells in the lung tissue was consistent with the increased VACV burden in these mice (Figure 1F).

Efficient CD8⁺ T cell-mediated immune surveillance in infected tissues requires a high density of responders (Halle et al., 2016), with an estimate of $\sim 3,000$ T_{RM} cells per million nucleated cells in the lungs (Steinert et al., 2015). Hence, we hypothesized that the highly abundant IST T_{RM} cells, in comparison to ~ 500 AW T_{RM} cells, participated in the rapid control of the infection established with $\sim 10^5$ PFU VACV that spreads through $\sim 2 \times 10^6$ alveoli. To test this hypothesis, we attempted adoptive transfer or selective local depletion of AW or IST T_{RM} cells before VACV challenge. We could not repopulate the lungs with a physiological density of endogenous epitope-specific IST T_{RM} cells because of poor yields (Steinert et al., 2015) and poor homing efficiency (data not shown). IN application of α CD8 Ab depleted AW T_{RM} cells as expected (Slütter et al., 2013), but significantly reduced IST T_{RM} as well (Figures S2C–S2E). As an alternative approach, we repopulated the airways of IP-vaccinated mice with ~ 770 B8R-specific AW T_{RM} cells per lung, which approximates two times their physiological number, harvested from intranasally vaccinated and VACV-challenged mice. The transferred AW T_{RM} cells neither egressed into the lung parenchyma nor provided resistance to VACV infection (Figure S5). Together these data suggest that IST T_{RM} cells elicited by IN, but not intraperitoneal, vaccination conferred early virus control and enhanced protection.

To determine why the pre-existing systemic memory CD8⁺ T cells accumulated slowly in the infected lungs, we assessed their proliferation kinetics. For this, IP-vaccinated mice were intranasally challenged with VACV and then pulsed with EdU

(5-ethynyl-2'-deoxyuridine) for 1 day. B8R-specific AW and IST T_{RM} cells showed modest EdU incorporation by day 4 p.i. and profound incorporation by day 6 p.i. By contrast, proliferation of B8R-specific blood, splenic, and lung MV CD8⁺ T cells was obvious only by day 6 p.i. (Figure 4B). Although it is likely that memory CD8⁺ T cells were proliferating in the draining LN at this time point (Moyron-Quiroz et al., 2006), proliferating cells were not detected in the blood and spleen until day 6 p.i. This result suggested that systemic CD8⁺ T cells had not yet left the LN to participate in viral clearance. The increased total number of B8R-specific IST T_{RM} cells in the lungs observed on day 4 p.i. was inversely related to ~ 3 - to 8-fold lower B8R-specific CD8⁺ T cells in blood, spleen, and lung vasculature (Figure 4C). Thus, the delayed recruitment of systemic resting memory CD8⁺ T cells to the lungs accounted for late accumulation of IST and AW T_{RM} cells during infection, which then extensively proliferated in situ.

By virtue of their location, IST T_{RM} cells can quickly engage in contact-dependent killing of infected lung tissue to confer enhanced immune protection, whereas MV CD8⁺ T cells are spatially isolated and cannot do so. To assess early activation of CD8⁺ T cell subsets in the lungs, intranasally immunized mice were challenged with VACV, and B8R epitope-specific MV CD8⁺ T cells (mostly CD69^{LO}) and IST T_{RM} (mostly CD69^{HI}) were assessed for CD69 induction within 36 hr p.i. Remarkably, only IST T_{RM} cells and not MV CD8⁺ T cells upregulated CD69 expression (Figure 4D), suggesting that IST T_{RM} cells are key initial responders to infection.

Interstitial T_{RM} Localize to Sites of the Lungs that Are Vulnerable to Infection

We previously showed that mortality in naive VACV-challenged mice was due to severe damage of alveoli characterized by widespread necrosis and fibrin-filled and edematous alveolar spaces (Gilchuk et al., 2013). Here, we determined the sites of VACV infection following IN inoculation with GFP reporter virus (Norbury et al., 2002) in conjunction with fluorescent labeling of type I alveolar epithelial cells with anti-rodoplanin Ab (Vanderbilt et al., 2008) on day 4 p.i. Confocal microscopy revealed that VACV localized to two spatially distinct niches surrounding the bronchioles and type I epithelial cells that form the alveolar walls (Figure 5A). Accordingly, imaging of α CD45 Ab⁻ CD8⁺ T cells in acutely infected lungs of vaccinated mice showed localization to the sites that are vulnerable to VACV infection, including the bronchioles and alveolar walls (Figure 5B).

Imaging of endogenous antigen-specific CD8⁺ T cells in the lungs was reported previously (Khanna et al., 2008; Moyron-Quiroz et al., 2006), but whether CD8⁺ T_{RM} cells occupy niches in the lung parenchyma where fatal infection occurs remains unknown. The pulmonary interstitium is the support tissue within the lungs; it includes the alveolar epithelium, capillary bed endothelium, basement membrane, and the perivascular and perilymphatic tissues. Collectively, they constitute the walls of the bronchioles and alveoli. To determine the location of VACV-specific IST T_{RM} cells, we stained thick fresh lung sections with fluorescent B8R tetramer (red) after IV labeling of vascular leucocytes with α CD45 Ab (blue) and vascular endothelium of alveolar capillary beds with fluorescent tomato lectin (green). Using selective

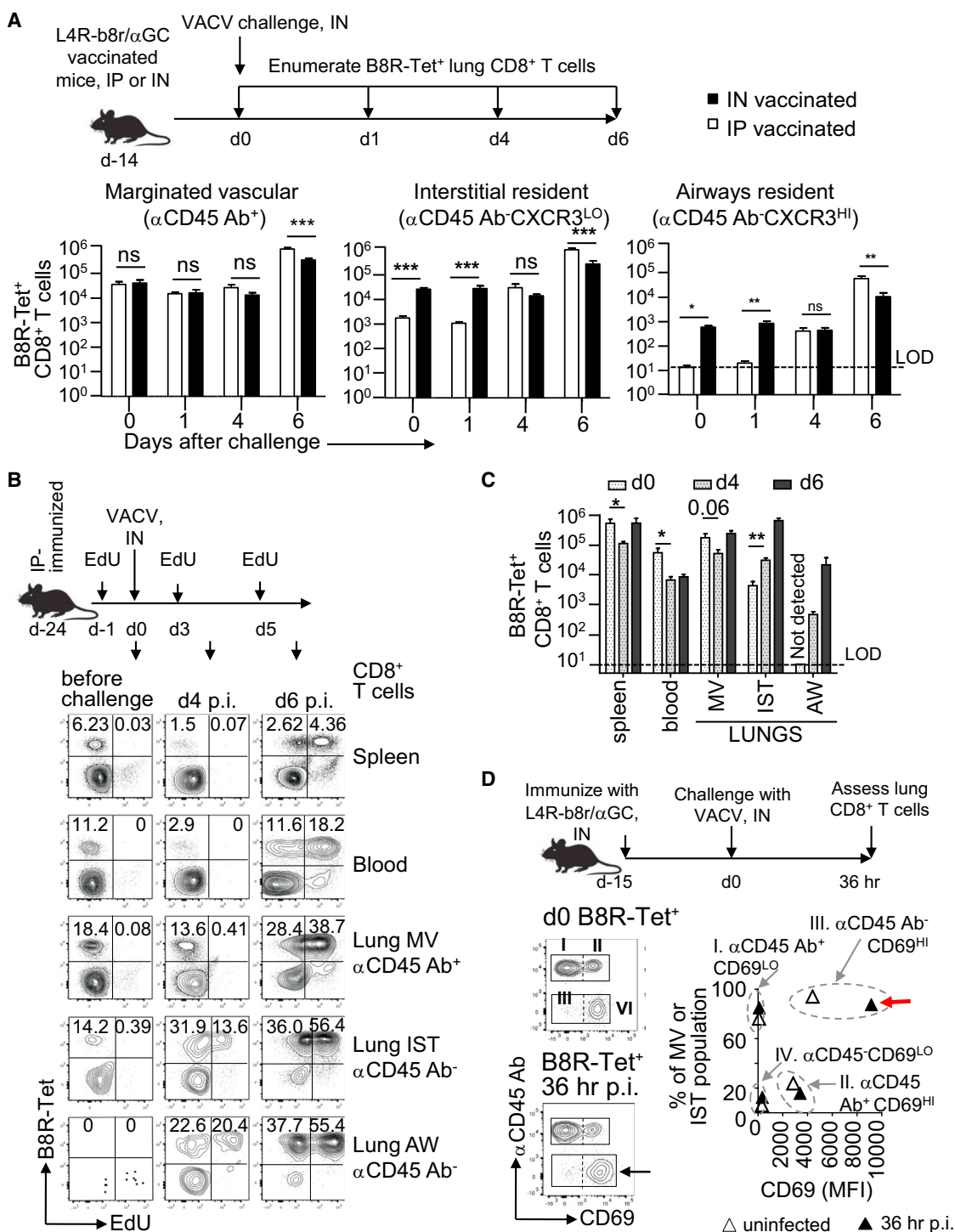


Figure 4. IST T_H Cells Persist in the Lungs and Respond before Systemic Memory CD8⁺ T Cells Accumulate to the Site of Infection

(A) Counts of B8R-specific MV, IST, and AW CD8⁺ T cells that were determined after intraperitoneal or IN vaccination (day 0) and at the indicated time points after IN challenge with VACV (n = 3–12 mice/group, mean \pm SEM).

(B) Proliferation kinetics of splenic, blood, and lung B8R-specific CD8⁺ T cells of IP-vaccinated mice was assessed by EdU incorporation at indicated time points p.i. Representative of three or four mice per group per time point.

(legend continued on next page)

plane illumination microscopy (SPIM), we achieved volumetric imaging that allowed visualization of VACV-specific CD8⁺ T cells in the alveolar interstitium (IST T_{RM}, red) and alveolar capillary beds (MV CD8⁺ T cells, magenta from the merge of red and blue) (see Figure 5C). We found that IN vaccination induced a substantial number of IST T_{RM} cells that localized within the alveolar walls, outside of alveolar capillaries (Figure 5C). Such a location of IST T_{RM} cells was even more prominent in acutely infected lungs of intranasally vaccinated mice, showing that infected alveoli are common sites of immune surveillance by IST T_{RM} cells that are located at the most vulnerable sites within the lung parenchyma.

DISCUSSION

At the internal barriers, the mucosal immune response confers the first line of defense against invading pathogens. Here, we report a distinct protective CD8⁺ T_{RM} cell that is elicited by IN protein antigen plus adjuvant vaccination and localized to the lungs interstitium, an anatomical site intimately connected to the respiratory mucosa. Sublethal respiratory infections induce bronchus-associated lymphoid tissue that serves as a site for naive CD8⁺ T cell priming and a niche for T_{RM} cell maintenance (Halle et al., 2009). Accordingly, IN infection with live influenza virus elicited a robust T_{RM} cell response that localized mostly around the large airways and blood vessels of the lungs (Wu et al., 2014). Other studies have suggested a protective role for CXCR3^{hi} memory CD8⁺ T cells also induced by viral infection but located within the airway lumen (McMaster et al., 2015; Slütter et al., 2013). Our findings extend the types of protective T_{RM} cells that patrol the lungs. Thus, in our IN protein antigen plus α GC adjuvant vaccination model, we identified a major CXCR3^{LO} IST T_{RM} cell subset that localizes to the most vulnerable sites of infection—the alveolar and bronchiolar walls. Efficient CD8⁺ T cell-mediated tissue surveillance depends on high responder density (Halle et al., 2016; Steinert et al., 2015). Accordingly, upon IN vaccination, IST T_{RM} cells were elicited at physiologically relevant numbers and accounted for most of the lung T_{RM} cells, suggesting these T_{RM} cells are key initial responders to infection. Nonetheless, at the late stages of infection, we do not discount the possibility that IST T_{RM} cells may replenish AW T_{RM} cells, which together with systemic effector memory CD8⁺ T cells may substantially contribute to the resolution of infection.

The mechanism by which CXCR3^{LO} IST T_{RM} cells are recruited and preferentially retained in the lung interstitium upon vaccination remains unclear. In this regard, our preliminary transcriptome analysis of naive lung CD8⁺ T cells and purified IST T_{RM} cells revealed many differentially expressed genes that could be associated with trafficking and/or residence in non-lymphoid tissues, including *CCR7*, *Irf2*, *Cxcr6*, *Cxcr3*, *Klrg1*, *Klf2*, and

Slpr1 (P.G. and S.J., unpublished data). The role of these genes in IST T_{RM} cell recruitment, retention, and function awaits further study.

Devising vaccination strategies to elicit T_{RM} cells in barrier tissues by immunization through an accessible tissue, such as skin, is an important goal for human vaccine design (Park and Kupper, 2015). In this regard, it is noteworthy that vaccination with VACV or replication-deficient modified vaccinia virus Ankara by skin scarification elicited memory CD8⁺ T cells that protected mice from lethal respiratory infection, although inactivated viruses failed to do so (Liu et al., 2010). Local immunization with CD8⁺ T cell-targeted epitope plus adjuvant could be a promising alternative to distal vaccination approach that uses virus vectors. Future studies will determine if vaccination by skin scarification with subunit vaccine formulation have the potential to elicit protective T_{RM} cells that also localize to distal barrier tissues. We hope our findings will have implications for the design of safe and effective CD8⁺ T cell-targeted vaccines against respiratory infections.

EXPERIMENTAL PROCEDURES

Mice, Viruses, and Antigens

B6-*K^DD⁰*;B*07;02^{tg} (B7^{tg}) transgenic mice have been described elsewhere (Alexander et al., 2003). Mouse breeding, maintenance, and experimentation complied with institutional animal care and use committee (IACUC) regulations.

The Western Reserve strain of VACV and VACV-GFP (a gift from J.W. Yewdell) were grown in and titrated with BSC-40 cells.

The design of recombinant L4R-derived antigen has been described elsewhere (Gilchuk et al., 2013). L4R-b8r DNA was generated by substituting the sequence that encodes FPRSMLSIF (L4R_{37–45}) in L4R_{33–249} DNA with a sequence that encodes FPKNDFVSF (B8R_{70–78}). Recombinant antigens were purified to high purity as described previously (Gilchuk et al., 2013).

Vaccination, Infections, and Burden

Ketamine-xylazine-anesthetized, 6- to 8-week-old mice were inoculated intranasally or intraperitoneally twice with 50 μ g antigenic protein formulated with 1 μ g α GC (Funakoshi) in 100 μ l PBS. To challenge, anesthetized mice were inoculated with 10⁵ PFU VACV in 50 μ l PBS. Mice were monitored daily for morbidity, and those losing over 30% of initial body weight were euthanized per IACUC regulations.

Lungs from individual mice were washed with PBS, homogenized, and subjected to one freeze/thaw cycle, and serial 10-fold dilutions were plated on confluent BSC-40 cells. Plaques were visualized by crystal violet staining.

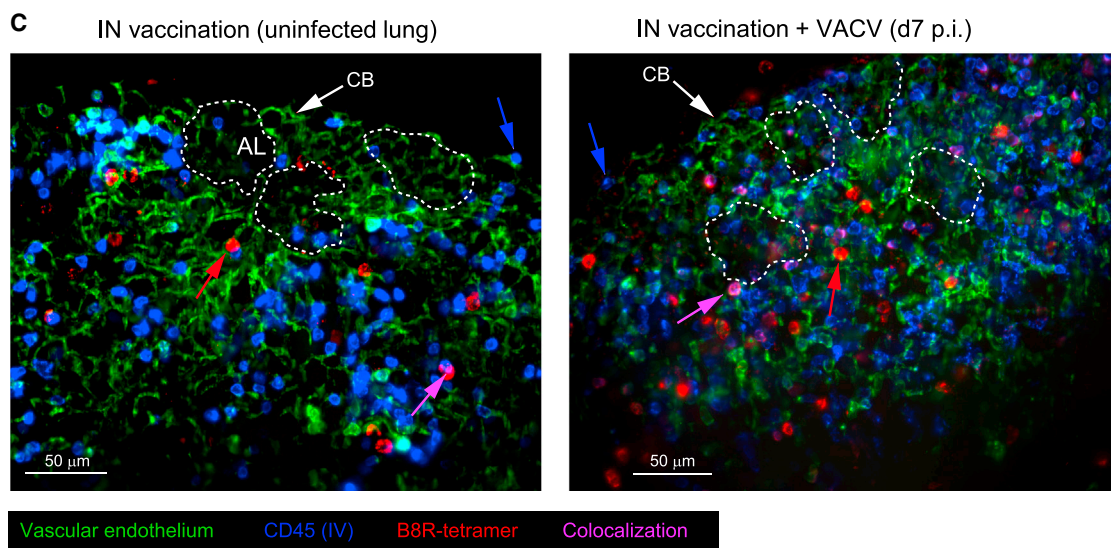
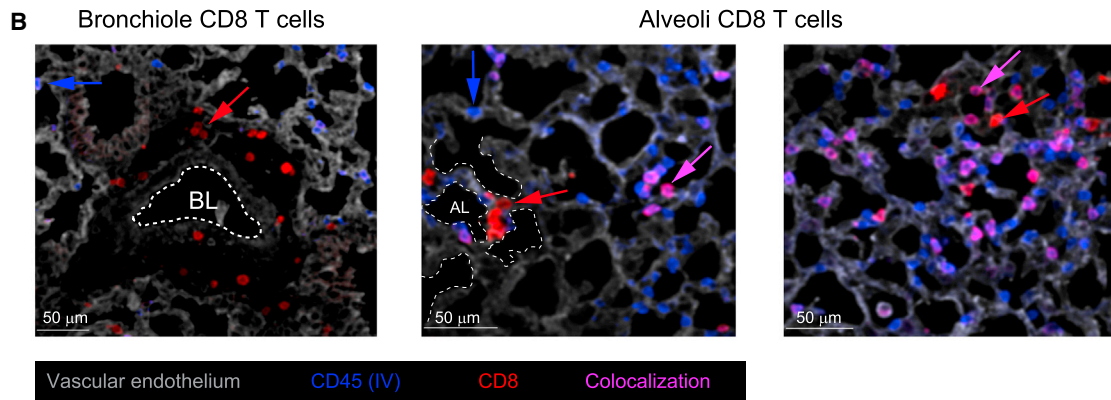
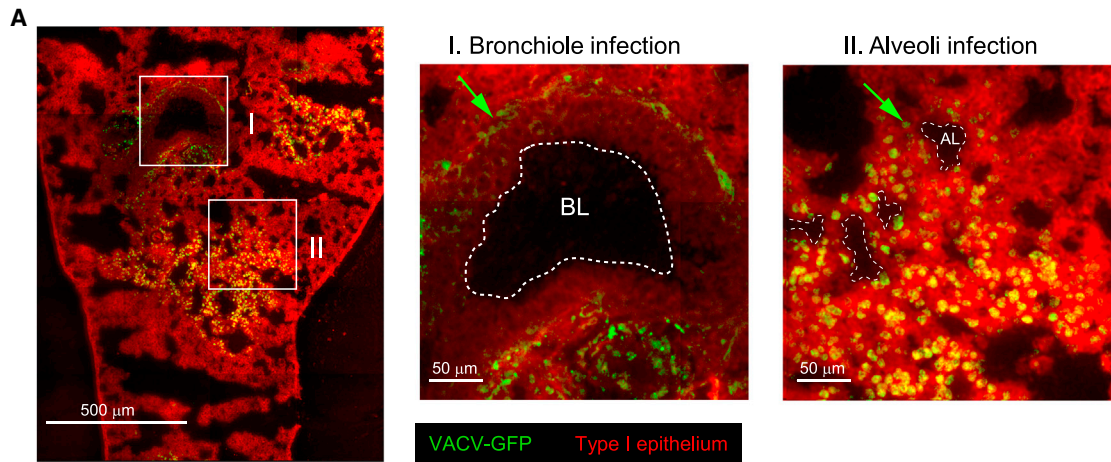
IV Staining and Flow Cytometry

IV staining was performed with fluorescently labeled α CD45 Ab as described previously (Anderson et al., 2014) but modified to precisely discriminate MV, AW, and IST CD8⁺ T cells. After IV staining, lungs were perfused, which removes cells from the vasculature and airway lumen while retaining MV and IST CD8⁺ T cells within the lung parenchyma. To account for BAL CD8⁺ T cells, the backflow from the airways, typically generated upon perfusion, was quantitatively recovered as detailed in the Supplemental Experimental Procedures.

(C) Number of Tet⁺ CD8⁺ T cells in spleen, blood, and lungs of mice vaccinated and challenged as in (B) was assessed at the indicated times (n = 3–4 mice/group, mean \pm SEM).

(D) Intranasally vaccinated mice were challenged with VACV or mock-inoculated with PBS (n = 4–5 mice/group). 36 hr p.i., Tet⁺ MV CD8⁺ T cells and IST T_{RM} cells were assessed for CD69 induction from pooled lungs in each group.

See also Figure S5.



(legend on next page)

In Vivo CD8⁺ T Cell Proliferation

Mice were injected with 1 mg EdU (Life Technologies) IP 24 hr before analysis. After IV staining, lung cells were labeled with viability dye to discriminate dead cells, followed by staining with tetramer and Abs. Cells were stained with Click-IT Plus EdU Alexa488 (Life Technologies) according to the manufacturer's protocol.

Confocal Microscopy and SPIM

For imaging of VACV-GFP, 10 μ m fresh-frozen lung sections were stained with α GFP-Alexa Fluor 488-conjugated Ab and mouse rodoanin Ab followed by secondary Alexa Fluor 647-conjugated Ab. For imaging of CD8⁺ T cells, lungs were harvested after IV staining with α CD45-BV421 Ab and fixed with 4% paraformaldehyde (PFA). Frozen 10 μ m sections were stained with α CD8⁺-PE Ab and AF488-labeled tomato lectin (Vector Laboratories). Confocal microscopy was performed using an AxioObserverZ.1 inverted microscope (Zeiss) equipped with a 20 \times 1.0 numerical aperture (NA) objective; 405-nm, 488-nm, and 561-nm laser lines; and dual sCMOS cameras. Image analysis was performed with Imlaris software (Bitplane Scientific). For imaging of B8R-specific CD8⁺ T cells in the lungs, mice were intravenously (i.v.) injected with AF488-labeled tomato lectin and α CD45-BV421 Ab, which visualizes vasculature and vascular leukocytes, respectively. Fresh, 1-mm-thick sections were cut with tissue slicer followed by overnight incubation with B8R tetramer-PE. Washed tissues were mounted in 1% agarose and analyzed using the LightsheetZ.1 platform (Zeiss) equipped with a CSU-22 spinning disc (Yokagawa), 473-nm and 660-nm laser lines, a 20–0.75 NA Plan-Apo objective, and an Evolve EMCCD camera (Photometrics). Images were analyzed using Slidebook software (Intelligent Imaging Innovations).

Statistics

Descriptive statistics (mean \pm SEM or mean \pm SD) are provided for continuous variables as noted. The Wilcoxon rank-sum test or two-sample t test was applied to two-group comparisons or the post hoc group comparisons in ANOVA; all tests were two tailed and unpaired (*p < 0.05; **p < 0.01; ***p < 0.001; ns, not significant). Statistical analyses were performed using the open source R software (version 2.15).

SUPPLEMENTAL INFORMATION

Supplemental Information includes Supplemental Experimental Procedures and five figures and can be found with this article online at <http://dx.doi.org/10.1016/j.celrep.2016.07.037>.

AUTHOR CONTRIBUTIONS

P.G., T.M.H., W.A.R., E.S., D.R.G., and S.J. conceived and designed experiments. P.G., T.M.H., and C.G. performed experiments. P.G., C.G., K.L.B., P.L., Y.S., and S.J. analyzed data. P.G., J.E.K., S.R.M., and S.J. wrote and edited the manuscript.

ACKNOWLEDGMENTS

We thank L. Van Kaer for critical evaluation of the data and review of the manuscript. This work was supported by a VA Merit Award (BX001444) to S.J.,

NIH contracts (AI040079), research (HL054977, AI042284, HL121139, and AI085062), training (GM007347), core (CA068485 and DK058404), and center (CA68485) grants, and a Mini-Sabbatical Award to P.G. from the Vanderbilt Immunology Center. SPIM microscopy images were acquired at the Cell & Tissue Imaging Center, which is supported by St. Jude Children's Research Hospital and P30 CA021765.

Received: September 25, 2015

Revised: April 14, 2016

Accepted: July 12, 2016

Published: August 4, 2016

REFERENCES

- Alexander, J., Oseroff, C., Sidney, J., and Sette, A. (2003). Derivation of HLA-B*0702 transgenic mice: functional CTL repertoire and recognition of human B*0702-restricted CTL epitopes. *Hum. Immunol.* *64*, 211–223.
- Anderson, K.G., Sung, H., Skon, C.N., Lefrancois, L., Deisinger, A., Vezys, V., and Masopust, D. (2012). Cutting edge: intravascular staining redefines lung CD8 T cell responses. *J. Immunol.* *189*, 2702–2706.
- Anderson, K.G., Mayer-Barber, K., Sung, H., Beura, L., James, B.R., Taylor, J.J., Qunaj, L., Griffith, T.S., Vezys, V., Barber, D.L., and Masopust, D. (2014). Intravascular staining for discrimination of vascular and tissue leukocytes. *Nat. Protoc.* *9*, 209–222.
- Ariotti, S., Beltman, J.B., Chodaczek, G., Hoekstra, M.E., van Beek, A.E., Gomez-Eerland, R., Ritsma, L., van Rheenen, J., Marée, A.F., Zal, T., et al. (2012). Tissue-resident memory CD8⁺ T cells continuously patrol skin epithelia to quickly recognize local antigen. *Proc. Natl. Acad. Sci. USA* *109*, 19739–19744.
- Barletta, K.E., Cagnina, R.E., Wallace, K.L., Ramos, S.I., Mehrad, B., and Linden, J. (2012). Leukocyte compartments in the mouse lung: distinguishing between marginated, interstitial, and alveolar cells in response to injury. *J. Immunol. Methods* *375*, 100–110.
- Bergsbaken, T., and Bevan, M.J. (2015). Proinflammatory microenvironments within the intestine regulate the differentiation of tissue-resident CD8⁺ T cells responding to infection. *Nat. Immunol.* *16*, 406–414.
- Bivas-Benita, M., Gillard, G.O., Bar, L., White, K.A., Webby, R.J., Hovav, A.H., and Letvin, N.L. (2013). Airway CD8(+) T cells induced by pulmonary DNA immunization mediate protective anti-viral immunity. *Mucosal Immunol.* *6*, 156–166.
- Clark, R.A. (2015). Resident memory T cells in human health and disease. *Sci. Transl. Med.* *7*, 269rv1.
- Courtney, A.N., Thapa, P., Singh, S., Wishahy, A.M., Zhou, D., and Sastry, J. (2011). Intranasal but not intravenous delivery of the adjuvant α -galactosylceramide permits repeated stimulation of natural killer T cells in the lung. *Eur. J. Immunol.* *41*, 3312–3322.
- Gilchuk, P., Spencer, C.T., Conant, S.B., Hill, T., Gray, J.J., Niu, X., Zheng, M., Erickson, J.J., Boyd, K.L., McAfee, K.J., et al. (2013). Discovering naturally processed antigenic determinants that confer protective T cell immunity. *J. Clin. Invest.* *123*, 1976–1987.
- Halle, S., Dujardin, H.C., Bakocevic, N., Fleige, H., Danzer, H., Willenzon, S., Suezter, Y., Hämmerling, G., Garbi, N., Sutter, G., et al. (2009). Induced

Figure 5. Protective TRM Cells Localize to Sites of the Lungs that Are Vulnerable to Infection

(A) Confocal image of VACV infection in lower airways and alveoli. Lungs of mice (n = 3) inoculated with VACV-GFP intranasally were harvested on day 4 p.i. to visualize infection sites. Left image is a composite of 20 \times objective images, with a maximum intensity projection of the z stack. Anti-rodoanin Ab stained for type I epithelium (red); VACV (green). Bronchiole lumen (BL) and alveolar lumen (AL) are shown with dotted lines.

(B) Confocal image of CD8⁺ IV α CD45 Ab⁺ (MV, magenta arrow), and CD8⁺ α CD45 Ab⁻ (IST; red arrow) T cells in the lung parenchyma. Lungs were harvested on day 7 after IN VACV challenge of IN prime boosted mice after IV staining with α CD45 Ab. Fixed 10- μ m lung sections were stained for CD8⁺ T cells. Vascular endothelium is gray, vascular leukocytes are blue, and CD8⁺ and IV α CD45 Ab⁺ T cells are magenta.

(C) Volumetric image of Tet⁺ IV α CD45 Ab⁺ (MV, magenta arrow) and Tet⁺ IV α CD45 Ab⁻ (IST, red arrow) B8R-specific CD8⁺ T cells in the lung alveoli. Perfused lungs were harvested on day 14 after IN boost with L4R-b8r (left) or day 7 after IN VACV challenge (right) of IN prime boosted mice. IV staining with fluorescently labeled tomato lectin and α CD45 Ab visualizes alveolar capillary beds and vascular leukocytes, respectively; in situ tetramer staining visualizes B8R-specific CD8⁺ T cells. Vascular endothelium is green, vascular leukocytes are blue, and Tet⁺ and α CD45 Ab⁺ CD8⁺ T cells are magenta; CB, capillary beads. Data are representative of two or three imaging areas of three or four sections per lung of two mice from two independent experiments per condition. Scale bar sizes are as indicated in each image.

- bronchus-associated lymphoid tissue serves as a general priming site for T cells and is maintained by dendritic cells. *J. Exp. Med.* 206, 2593–2601.
- Halle, S., Keyser, K.A., Stahl, F.R., Busche, A., Marquardt, A., Zheng, X., Galla, M., Heissmeyer, V., Heller, K., Boelter, J., et al. (2016). In vivo killing capacity of cytotoxic T cells is limited and involves dynamic interactions and T cell cooperativity. *Immunity* 44, 233–245.
- Hasenberg, M., Stegemann-Koniszewski, S., and Gunzer, M. (2013). Cellular immune reactions in the lung. *Immunol. Rev.* 251, 189–214.
- Hickman, H.D., Reynoso, G.V., Ngudiankama, B.F., Cush, S.S., Gibbs, J., Bennink, J.R., and Yewdell, J.W. (2015). CXCR3 chemokine receptor enables local CD8(+) T cell migration for the destruction of virus-infected cells. *Immunity* 42, 524–537.
- Jiang, X., Clark, R.A., Liu, L., Wagers, A.J., Fuhlbrigge, R.C., and Kupper, T.S. (2012). Skin infection generates non-migratory memory CD8+ T(RM) cells providing global skin immunity. *Nature* 483, 227–231.
- Khanna, K.M., Aguila, C.C., Redman, J.M., Suarez-Ramirez, J.E., Lefrançois, L., and Cauley, L.S. (2008). In situ imaging reveals different responses by naïve and memory CD8 T cells to late antigen presentation by lymph node DC after influenza virus infection. *Eur. J. Immunol.* 38, 3304–3315.
- Kohlmeier, J.E., Cookenham, T., Miller, S.C., Roberts, A.D., Christensen, J.P., Thomsen, A.R., and Woodland, D.L. (2009). CXCR3 directs antigen-specific effector CD4+ T cell migration to the lung during parainfluenza virus infection. *J. Immunol.* 183, 4378–4384.
- Leikes, E., Headley, M.B., Thornton, E.E., Looney, M.R., and Krummel, M.F. (2014). The spatiotemporal cellular dynamics of lung immunity. *Trends Immunol.* 35, 379–386.
- Li, A.V., Moon, J.J., Abraham, W., Suh, H., Elkhader, J., Seidman, M.A., Yen, M., Im, E.J., Foley, M.H., Barouch, D.H., and Irvine, D.J. (2013). Generation of effector memory T cell-based mucosal and systemic immunity with pulmonary nanoparticle vaccination. *Sci. Transl. Med.* 5, 204ra130.
- Liu, L., Zhong, Q., Tian, T., Dubin, K., Athale, S.K., and Kupper, T.S. (2010). Epidermal injury and infection during poxvirus immunization is crucial for the generation of highly protective T cell-mediated immunity. *Nat. Med.* 16, 224–227.
- Mackay, L.K., Rahimpour, A., Ma, J.Z., Collins, N., Stock, A.T., Hafon, M.L., Vega-Ramos, J., Lauzurica, P., Mueller, S.N., Stefanovic, T., et al. (2013). The developmental pathway for CD103(+)CD8+ tissue-resident memory T cells of skin. *Nat. Immunol.* 14, 1294–1301.
- Manicassamy, B., Manicassamy, S., Belicha-Villanueva, A., Pisanelli, G., Puelandran, B., and Garcia-Sastre, A. (2010). Analysis of in vivo dynamics of influenza virus infection in mice using a GFP reporter virus. *Proc. Natl. Acad. Sci. USA* 107, 11531–11536.
- McMaster, S.R., Wilson, J.J., Wang, H., and Kohlmeier, J.E. (2015). Airway-resident memory CD8 T cells provide antigen-specific protection against respiratory virus challenge through rapid IFN- γ production. *J. Immunol.* 195, 203–209.
- Moyron-Quiroz, J.E., Rangel-Moreno, J., Hartson, L., Kusser, K., Tighe, M.P., Klonowski, K.D., Lefrançois, L., Cauley, L.S., Harmsen, A.G., Lund, F.E., and Randall, T.D. (2006). Persistence and responsiveness of immunologic memory in the absence of secondary lymphoid organs. *Immunity* 25, 643–654.
- Norbury, C.C., Malide, D., Gibbs, J.S., Bennink, J.R., and Yewdell, J.W. (2002). Visualizing priming of virus-specific CD8+ T cells by infected dendritic cells in vivo. *Nat. Immunol.* 3, 265–271.
- Park, C.O., and Kupper, T.S. (2015). The emerging role of resident memory T cells in protective immunity and inflammatory disease. *Nat. Med.* 21, 688–697.
- Rangel-Moreno, J., Carragher, D.M., de la Luz Garcia-Hernandez, M., Hwang, J.Y., Kusser, K., Hartson, L., Kolls, J.K., Khader, S.A., and Randall, T.D. (2011). The development of inducible bronchus-associated lymphoid tissue depends on IL-17. *Nat. Immunol.* 12, 639–646.
- Salek-Ardakani, S., Moutaftsi, M., Sette, A., and Croft, M. (2011). Targeting OX40 promotes lung-resident memory CD8 T cell populations that protect against respiratory poxvirus infection. *J. Virol.* 85, 9051–9059.
- Schenkel, J.M., and Masopust, D. (2014). Tissue-resident memory T cells. *Immunity* 41, 886–897.
- Schenkel, J.M., Fraser, K.A., Beura, L.K., Pauken, K.E., Vezyz, V., and Masopust, D. (2014). T cell memory. Resident memory CD8 T cells trigger protective innate and adaptive immune responses. *Science* 346, 98–101.
- Semmling, V., Lukacs-Kornek, V., Thaiss, C.A., Quast, T., Hochheiser, K., Panzer, U., Rossjohn, J., Perlmutter, P., Cao, J., Godfrey, D.I., et al. (2010). Alternative cross-priming through CCL17-CCR4-mediated attraction of CTLs toward NKT cell-licensed DCs. *Nat. Immunol.* 11, 313–320.
- Sheridan, B.S., Pham, Q.M., Lee, Y.T., Cauley, L.S., Puddington, L., and Lefrançois, L. (2014). Oral infection drives a distinct population of intestinal resident memory CD8(+) T cells with enhanced protective function. *Immunity* 40, 747–757.
- Shin, H., and Iwasaki, A. (2012). A vaccine strategy that protects against genital herpes by establishing local memory T cells. *Nature* 497, 463–467.
- Slütter, B., Pewe, L.L., Kaech, S.M., and Harty, J.T. (2013). Lung airway-surveillance CXCR3(hi) memory CD8(+) T cells are critical for protection against influenza A virus. *Immunity* 39, 939–948.
- Steinert, E.M., Schenkel, J.M., Fraser, K.A., Beura, L.K., Manlove, L.S., Igyártó, B.Z., Southern, P.J., and Masopust, D. (2015). Quantifying memory CD8 T cells reveals regionalization of immunosurveillance. *Cell* 161, 737–749.
- Takamura, S., Roberts, A.D., Jelley-Gibbs, D.M., Wittmer, S.T., Kohlmeier, J.E., and Woodland, D.L. (2010). The route of priming influences the ability of respiratory virus-specific memory CD8+ T cells to be activated by residual antigen. *J. Exp. Med.* 207, 1153–1160.
- Vanderbilt, J.N., Allen, L., Gonzalez, R.F., Tigue, Z., Edmondson, J., Ansaldo, D., Gillespie, A.M., and Dobbs, L.G. (2008). Directed expression of transgenes to alveolar type I cells in the mouse. *Am. J. Respir. Cell Mol. Biol.* 39, 253–262.
- Wu, T., Hu, Y., Lee, Y.T., Bouchard, K.R., Benechet, A., Khanna, K., and Cauley, L.S. (2014). Lung-resident memory CD8 T cells (TRM) are indispensable for optimal cross-protection against pulmonary virus infection. *J. Leukoc. Biol.* 95, 215–224.

Cell Reports, Volume 16

Supplemental Information

A Distinct Lung-Interstitial-Resident Memory CD8⁺

T Cell Subset Confers Enhanced Protection

to Lower Respiratory Tract Infection

Pavlo Gilchuk, Timothy M. Hill, Clifford Guy, Sean R. McMaster, Kelli L. Boyd, Whitney A. Rabacal, Pengcheng Lu, Yu Shyr, Jacob E. Kohlmeier, Eric Sebzda, Douglas R. Green, and Sebastian Joyce

Figure S1 – Related to Figure 1

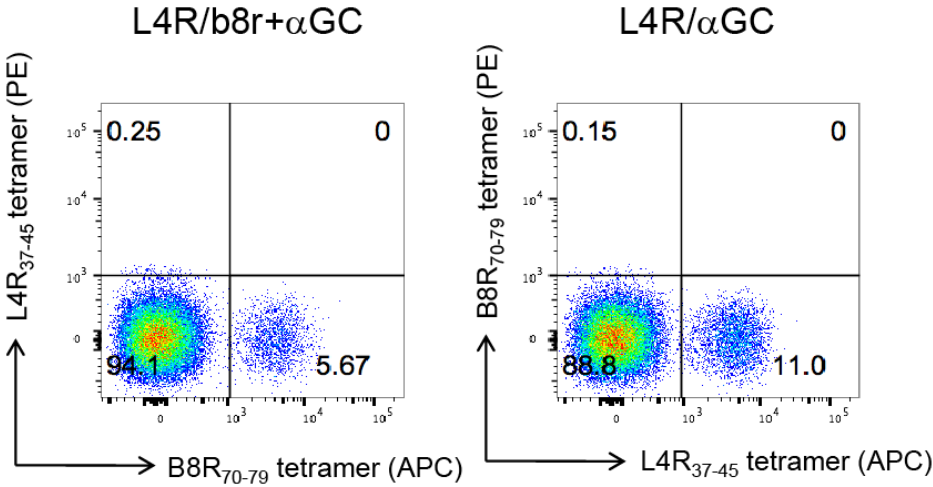


Figure S2 – Related to Figure 2

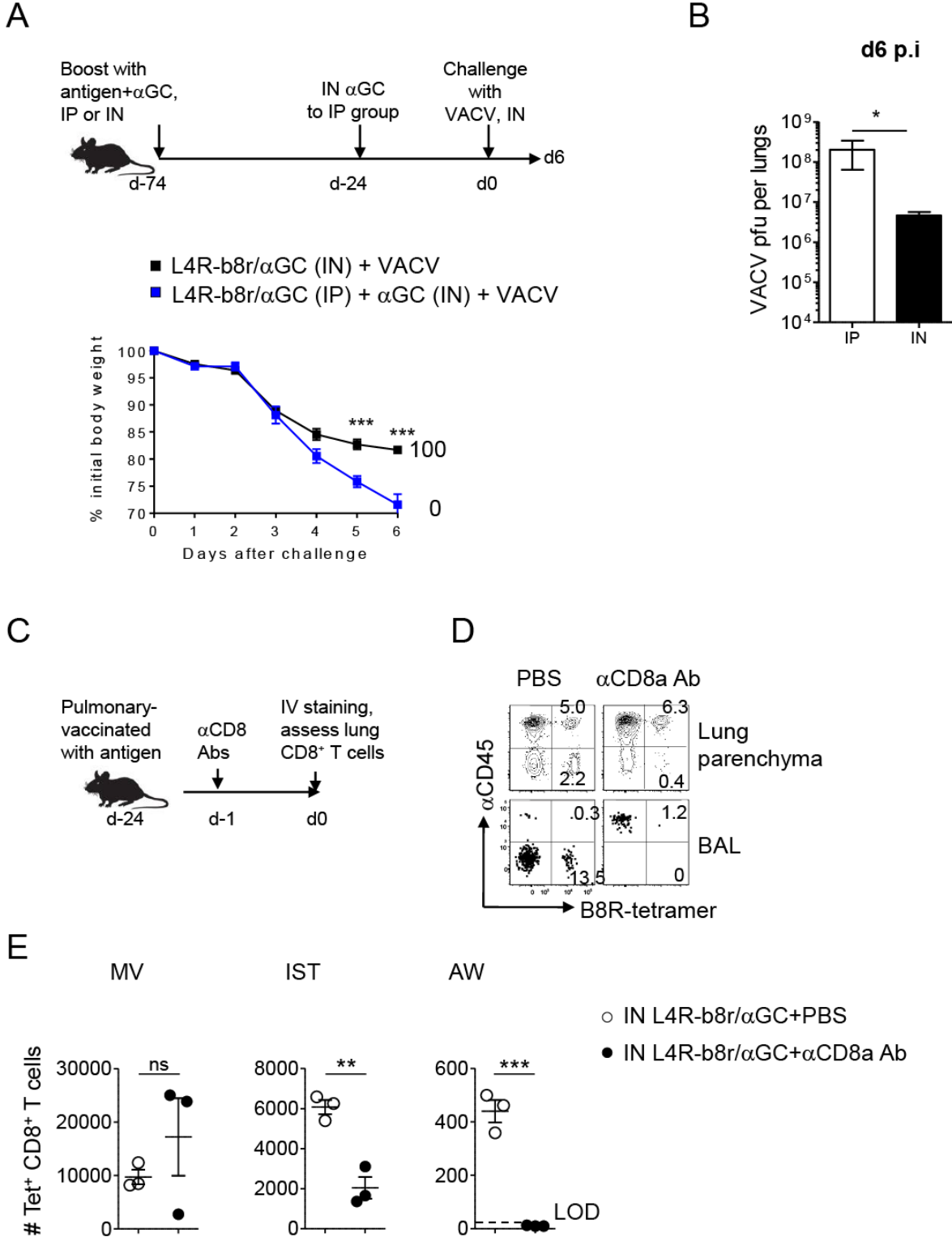
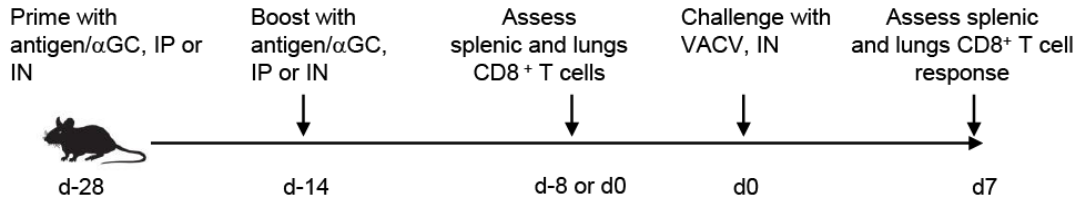


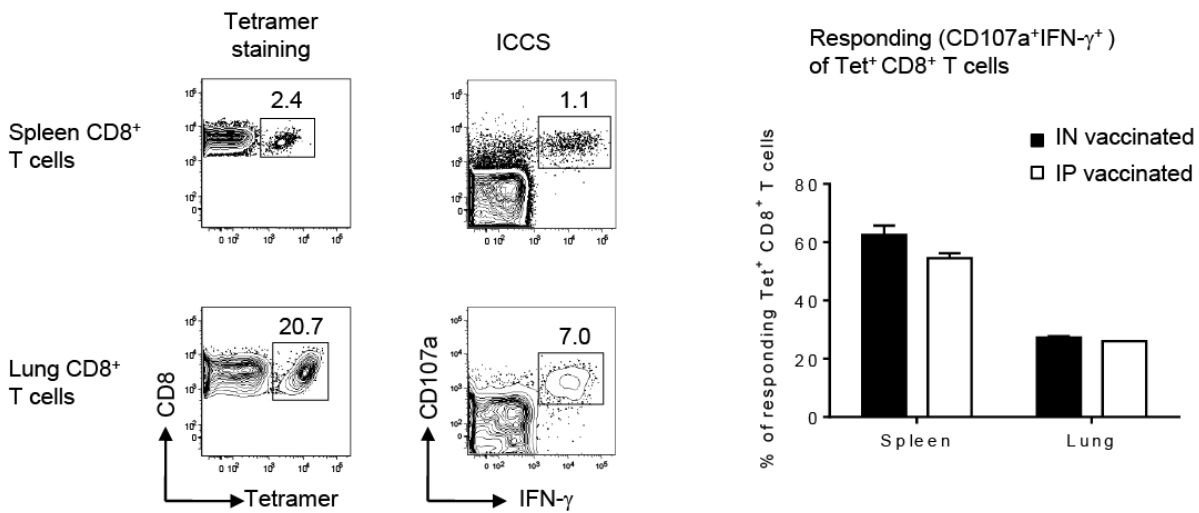
Figure S3 – Related to Figure 3

A



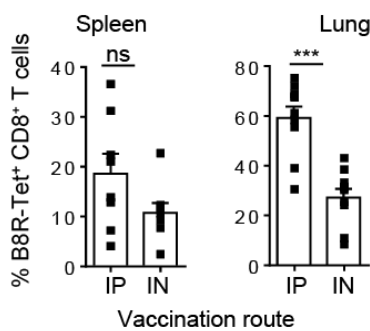
B

Post vaccination (d0)



C

After VACV challenge (d7 p.i.)



D

After VACV challenge (d7 p.i.)

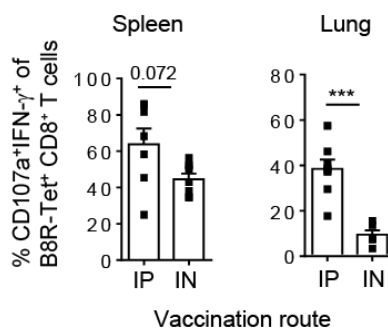
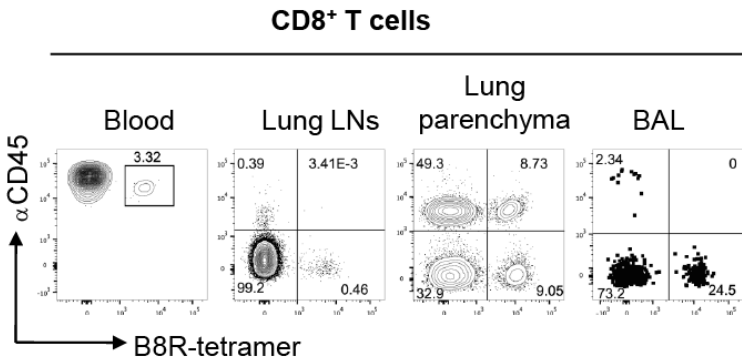
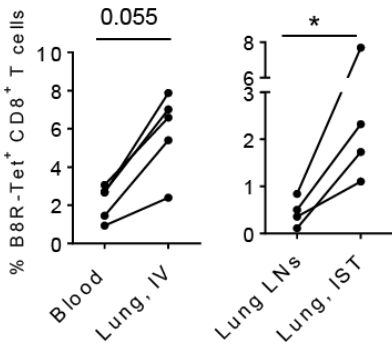


Figure S4 – Related to Figure 3

A



B



C

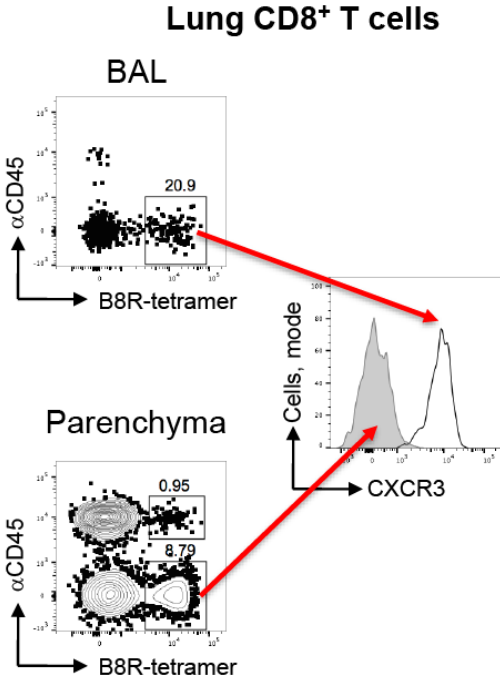
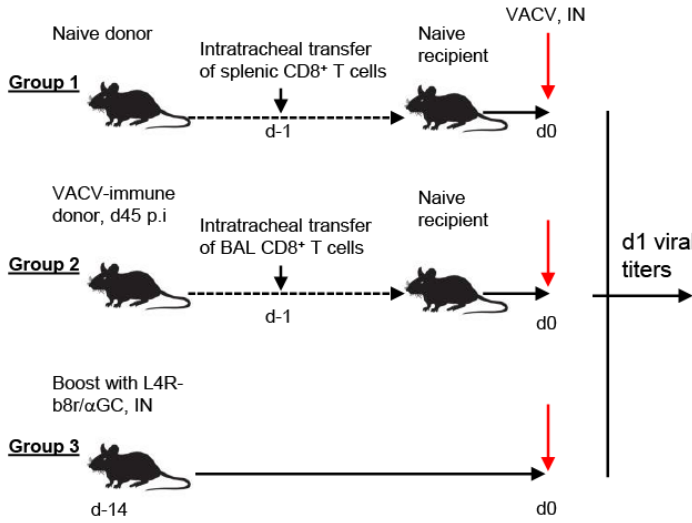
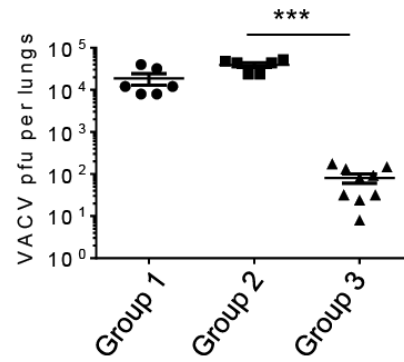


Figure S5 – Related to Figure 4

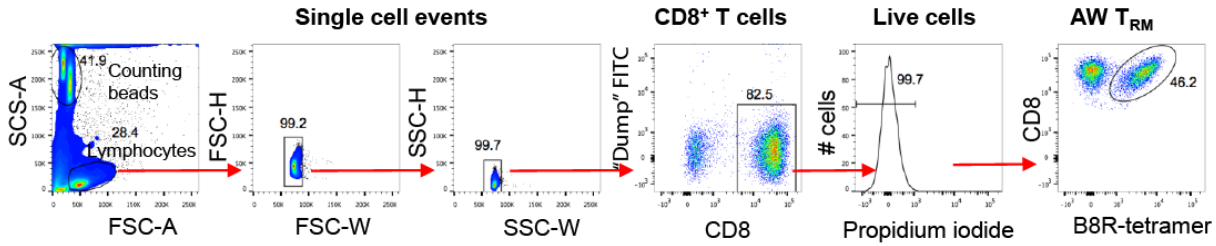
A



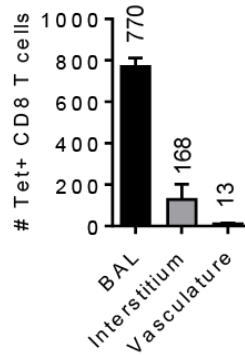
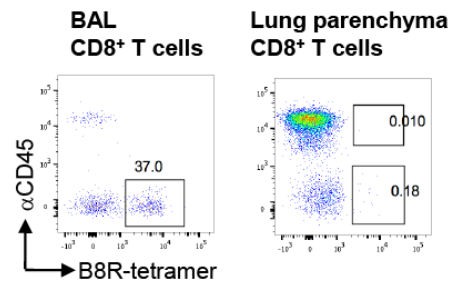
B



C



D



E

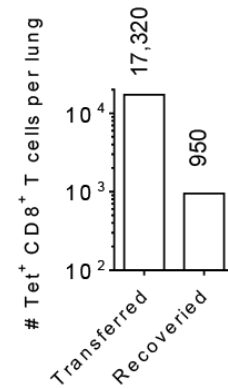


Figure S1. Adjuvant plus protein antigen prime and boost elicited memory CD8⁺ T cells are reactive only to the homologous epitope of protein that was used for immunization –Related to Figure 1

Mice were primed and boosted with L4R or L4R-b8r protein and adjuvant by intranasal route. Lungs were harvested on day 6 after the boost. Epitope-specific CD8⁺ T cells for each immunized group were assessed in same staining reaction with two, homologous or heterologous, tetramers which are labeled with PE or APC as indicated. Data represent one of two or three mice for each group. Plots are gated on live CD8⁺ T cells.

Figure S2. CD8⁺ T cells induced by IN vaccination participate in protection –Related to Figure 2

(A–B). IN α GC treatment of IP vaccinated mice did not protect mice from lethal VACV challenge on d24 after the treatment. Mice were immunized IN or IP with L4r-b8r plus α GC. On d50 after boost, IP vaccinated mice were administered α GC IN. On d24 after IN α GC administration, i.e., d74 after boost, both groups were challenged with VACV and monitored for protection by assessing weight loss kinetics (A) and virus titers in the lungs on d6 after challenge (B). One of two independent experiments are shown, $n=3$ –5 mice per group; mean \pm SEM. Number indicates % survival based on endpoint criteria.

(C–E) IN vaccinated mice are more susceptible to VACV after local depletion of CD8⁺ T cells.

(C) IN vaccinated mice received 5 μ g α CD8 Ab or PBS IN. CD8⁺ T cells were assessed in the lungs after 24h. IV staining with CD45 Ab followed by tetramer staining were used to discriminate TRM in the lungs.

(D) Representative flow plots show gates for CD8⁺ T cells of mice that were treated with PBS or α CD8 Ab as in (C).

(E) Quantification of CD8⁺ T cell subsets from mice treated as in (C). ($n=3$ per group); mean \pm SEM. AW: airway, MV: margined vascular, IST: interstitial resident CD8⁺ T cells.

Figure S3. Frequency and functional competence of epitope-specific CD8⁺ T cells that generated via IN and IP vaccinations –Related to Figure 3

(A) Schema of immunization and CD8⁺ T cell analysis.

(B) Responsiveness of B8R-specific CD8⁺ T cells that generated by IN or IP vaccination to peptide re-stimulation in vitro. Splens or lungs were harvested on d6 or d14 after boost with L4R-b8r and α GC and split into two separate reactions, which included tetramer staining, or re-stimulation with B8R peptide followed by intracellular IFN- γ and CD107a staining (ICCS). Representative flow cytometry plots are shown for spleen and lungs of IN vaccinated mice (left panel) and percent of responding antigen-specific CD8⁺ T cells CD107a⁺IFN- γ ⁺ cells (right panel) that calculated as fraction of Tet⁺ CD8⁺ T cells. One of two independent experiments with pooled splens or lungs ($n=3$). Mean \pm SD of assay triplicates.

(C). Frequency of B8R-specific CD8⁺ T cells identified by tetramer staining in lungs and spleen of IP or IN vaccinated mice on d7 after IN VACV challenge.

(F) Frequency of IFN- γ ⁺ CD107a⁺ B8R epitope-specific CD8⁺ T cells from (C) that calculated as in (B). Each symbol indicates an individual mouse, $n=6$ –10 mice/group; mean \pm SEM.

Figure S4. Feasibility of the approach to discriminate different CD8⁺ T cell subsets in the lungs –Related to Figure 3

Mice ($n=4$ –5) were immunized IN with L4r-b8r plus α GC. Lungs parenchyma, BAL, blood, and mediastinal lymph nodes were harvested for the analysis on d8-14 after the boost. IV staining with CD45 Ab followed by tetramer staining were used to discriminate T_{RM}.

Representative flow cytometry plots (A) and frequency (B) showing feasibility of the approach to identify different immune CD8⁺ T cells in the lungs. Each connecting line on (B) represents individual mouse.

(C) Representative flow cytometry plots showing discrimination of IST and AW TRM by CXCR3 staining.

Figure S5. Low number of AW T_{RM} could not account for the rapid virus control in infected lungs –Related to Figure 4

(A) Experimental design. Fourteen mice were primed and boosted IN with L4R-b8r protein and α GC and then inoculated IN with VACV. On day 45 p.i. BAL CD8⁺ T cells were purified by magnetic sorting, counted and adoptively transferred by intra-tracheal route to non-immune recipient mice ($n=9$) in 100 μ l of sterile PBS. Each mouse received \sim 17,000 of alive B8R-specific AW T_{RM}. Other group ($n=6$) received \sim 30,000 of purified naïve splenic CD8⁺ T cells. Third group ($n=9$) that were primed and boosted IN with L4R-b8r protein and α GC served as positive control for protection. Twenty-four hours after transfer mice were challenged IN with VACV.

(B) Virus titers assessed 24 hours p.i in the lungs of individual mice from (A).

(C) Aliquot of magnetically purified recipients BAL CD8⁺ T cells that were used for adoptive transfer. Gating strategy to identify count viable B8R-epitope specific AW TRM is shown.

(D–E) Repopulation efficiency of the airways after adoptive intra-tracheal transfer of airway resident memory CD8⁺ T cells. BAL and lungs parenchyma of three donor mice were assessed for B8R-specific AW TRM 24 hours after adoptive transfer. The efficiency of the

airway repopulation/recovery of adoptively transferred AW TRM is ~5% (mean 770 cells per mouse lungs) which is approximately two-fold excess of their physiological number upon protein antigen and adjuvant vaccination (mean 495 cells per mouse lungs).

Supplemental Experimental Procedures

IV staining and flow cytometry

Mice were injected i.v. with 2 μ g fluorescently labeled α CD45 Ab and after 5 min, lungs were slowly perfused with 10ml PBS to ensure blood removal before lungs inflation. AW CD8⁺ T cells was quantitatively collected with the backflow (3—5ml) from the airways typically generated after lung inflation. Of note, recent study suggested avoiding lung perfusion to preserve airway resident populations (Anderson et al., 2014) although for our study lung perfusion was required to minimize contamination of IST TRM with α CD45- AW TRM for phenotyping analysis. Collagenase-digested lung was used without further purification for CD8⁺ T cells assays and counting. For direct ex vivo intracellular staining, lungs were processed in presence of 10 μ g/ml brefeldin A (Sigma). For in vitro re-stimulation assays, cells were incubated with 10 μ g/ml of antigenic peptide and α CD107a Ab as described (Gilchuk et al., 2013). CD8⁺ T cells counting was performed with counting beads as described (Gilchuk et al., 2013). Preparation of fluorescent tetramers and CD8⁺ T cells staining were described previously (Gilchuk et al., 2013). Dead cells were discriminated using viability dye Flow cytometric data were collected using an LSRII (BD Biosciences) and analyzed with FlowJo software (Tree Star, Ashland, OR).

CD8 depletion

Local depletion of CD8⁺ T cells in lung was performed as described previously (Slutter et al., 2013). Briefly, 5 μ g of anti-CD8 α antibody (clone 2.43) was administrated in 50 μ l of sterile PBS by intranasal route to anesthetized mice, and after 24h CD8⁺ T cells were assessed in different lung compartments with tetramer. Mock (PBS)-treated mice served as a baseline control for CD8⁺ T cells counting, and for VACV challenge experiments.

Intra-tracheal transfer of AW TRM

Isolation and adoptive transfer of AW TRM were performed as described previously (McMaster et al., 2015). Briefly, mice were primed and boosted IN with L4R-b8r protein and α GC and then inoculated IN with VACV. On day 45 p.i. BAL CD8⁺ T cells were purified using a Miltenyi Biotec CD8 α T cell isolation kit II, counted and adoptively transferred by intra-tracheal route to non-immune recipient mice in 100 μ l of sterile PBS.

Flow cytometry and microscopy reagents

Tetramers

B8R₇₀₋₇₉ (FPKNDVVSF)/HLA-B7.2 PE
B8R₇₀₋₇₉ (FPKNDVVSF)/HLA-B7.2 APC
B8R₇₀₋₇₉ (FPKNDVVSF)/HLA-B7.2 BV421
NP₃₆₆₋₃₇₄ (ASNENMETM)/H2D^b PE
L4R₃₇₋₄₅ (FPRSMLSIF)/B7.2 PE

Antibodies

Anti-CD8 α -APC-Cy7 (clone 53-6.7; BD Biosciences, San Jose, CA)
Anti-IL-2-PE (clone JES6-5H4; BD Biosciences)
Anti-CD44-APC (clone IM7; BD Biosciences)
Anti-CD62L-APC-Cy7 (clone MEL-14; BD Biosciences)
Anti-CD45-BV421 (clone 30-F11; BD Biosciences)
Anti-CD8 α -PerCP-Cy5.5 (clone 53-6.7; BD Biosciences)
Anti-CD3 ϵ -PE (clone 145-2C11; BD Biosciences)
Anti-B220-FITC (clone RA3-6B2; BD Biosciences)
Anti-B220-APC-Cy7 (clone RA3-6B2; BD Biosciences)
Anti-CD11c-FITC (clone N418; Tonbo Biosciences, San Diego, CA)
Anti-B4-FITC (clone H129.19; BD Biosciences)
Anti-CD11b-FITC (clone M1/70; Tonbo Biosciences)
Anti-CD8 α -Pacific Blue (clone 53-6.7; BD Biosciences)
Anti-CD107a-FITC (clone 1D4B; BD Biosciences)
Anti-CD44-APC-Cy7 (clone IM7; BD Biosciences)
Anti-CCR7-PE (clone 4B12; BD Biosciences)
Anti-CD11a-FITC (clone 2D7; BD Biosciences)
Anti-KLRG1-APC (clone 2F1; eBioscience, San Diego, CA)
Anti-CD183 (CXCR3)-APC (clone CXCR3-173; BD Biosciences)
Anti-CD279 (PD-1)-PE (clone J43; BD Biosciences)
Anti-CD69-PerCP-Cy5.5 (clone H1.2F3; BD Biosciences)
Anti-CD45.2-APC (clone 104; BD Biosciences)
Anti-IFN- γ -APC (clone XMG1.2; BD Biosciences)
Anti-IFN- γ -PE (clone XMG1.2; BD Biosciences)
Anti-CD122-PE (clone TM- β 1; BioLegend, San Diego, CA)
Anti-CD103-PE (clone 2E7; BioLegend)
Anti-CD49b-PE (clone DX5; BioLegend)
Anti-CD43-PE (clone 1B11; BioLegend)
Anti-CD49b-PE (clone DX5; BioLegend)
Anti-CD27-PE (clone LG.3A10; BioLegend)
Anti-CD47-PE (clone miap301; BioLegend)
Anti-CD184 (CXCR4)-PE (clone L276F12; BioLegend)
Anti-CD49a-PE (clone Ha31/8; BioLegend)
Anti-CTLA-4-PE (clone UC10-4F10-11; Tonbo Biosciences)
Anti-TNF-PE (clone MP6-XT22; BD Biosciences)
Anti-CD4-FITC (clone RM4-4; BD Biosciences)
Anti-Granzyme B-PE (clone GB11; Life Technologies, Grand Island, NY)
Anti-Podoplanin unconjugated (clone 8.1.1; BioLegend)
Anti-GFP-Alexa Fluor 488 (rabbit polyclonal; Life Technologies)
Anti-Syrian Hamster IgG Alexa Fluor 647-conjugated (goat polyclonal; Jackson ImmunoResearch, West Grove, PA)

Viability dyes

Propidium iodide (BD Biosciences)
eFluor450 amino-reactive viability dye (eBioscience)

Other reagents

Brilliant Violet 421 streptavidin conjugate (BioLegend)

R-phycoerythrin (PE) streptavidin conjugate (Life Technologies)

Allophycocyanin (APC) streptavidin conjugate (Life Technologies)

DyLight 488 lycopersicon Esculentum (tomato) lectin (Vector Laboratories, Burlingame, CA)

Supplemental References

Anderson, K.G., Mayer-Barber, K., Sung, H., Beura, L., James, B.R., Taylor, J.J., Qunaj, L., Griffith, T.S., Vezys, V., Barber, D.L., *et al.* (2014). Intravascular staining for discrimination of vascular and tissue leukocytes. *Nat Protoc* *9*, 209-222.

Gilchuk, P., Spencer, C.T., Conant, S.B., Hill, T., Gray, J.J., Niu, X., Zheng, M., Erickson, J.J., Boyd, K.L., McAfee, K.J., *et al.* (2013). Discovering naturally processed antigenic determinants that confer protective T cell immunity. *The Journal of clinical investigation* *123*, 1976-1987.

McMaster, S.R., Wilson, J.J., Wang, H., and Kohlmeier, J.E. (2015). Airway-Resident Memory CD8 T Cells Provide Antigen-Specific Protection against Respiratory Virus Challenge through Rapid IFN-gamma Production. *J Immunol* *195*, 203-209.

Slutter, B., Pewe, L.L., Kaech, S.M., and Harty, J.T. (2013). Lung airway-surveilling CXCR3(hi) memory CD8(+) T cells are critical for protection against influenza A virus. *Immunity* *39*, 939-948.